Center for Astrophysics

Harvard College Observatory
Smithsonian Astrophysical Observatory

MEMORANDUM

March 12, 1998

To: S. Murray
From: G. Meehan

Subject: Calibration of the HRC Back-Up UV/Ion Shield Witness Samples
cc: M. Zombeck, A. Kenter, R. Kraft, D. Goddard, M. Juda, D. Pease, R. Donnelly

1 Introduction

In support of experimental activities related to the HRC program, x-ray transmission measurements were carried out on a series of UV/ion shield witness samples. Most of these samples are associated with the back-up flight UV/ion shields. However, two flight UV/ion shield witness samples that were previously measured at the BESSY synchrotron in Bonn, Germany were included in these tests. A sample of the window material used in x-ray pipe #1's Manson source monitor detector, a gas flow proportional counter, was also measured. This report is a summary of those measurements.

2 X-ray Monochromator Transmission Measurements

Every UV/ion shield supplied to us by the Luxel Corporation (Friday Harbor, WA) was accompanied by two witness samples, each of which is 16mm in diameter. Each pair of witness samples comes from the same production run as its associated UV/ion shield, and are taken from different regions of the larger shield sheet. The experimental setup precluded any effort to perform spatial uniformity measurements on a given witness sample. Rather, each measurement represents an average transmission over a filter. We know from previous uniformity measurements of candidate HRC-I UV/ion shields, however, that they are spatially uniform in transmission within 5% (relative) at a spatial scale of 1 mm.[1,2] All of the witness samples, as well as the proportional counter window sample, tested within this work are listed in table 1. Of the 9 witness samples, TF100-354 and TF101-891 are flight UV/ion shield witness samples that were tested previously at the PTB laboratory of the BESSY synchrotron in Bonn, Germany[3]. Included in this table are the thickness values of the constituent layers as reported by Luxel. Figure 1 shows the nominal thickness values of the HRC-I and HRC-S UV/ion shields.

3 Instrumental Setup

The transmission measurements were carried out at the SAO using a McPherson model 248/310G 1-meter diameter grazing incidence monochromator. It is equipped with a 1200 G/mm grating that has a $2^o5'$ blaze angle and a 5442 $\AA$ blaze wavelength, which yields an operating range of 2.8 $\AA$ to 340.7 $\AA$. The monochromator entrance and exit slits were set to a nominal 20 μm width to minimize contamination by the x-ray continuum. Figure 2 represents a typical monochromator beam scan to identify the fluorescent lines associated with the anode selected for use in the Manson model 2 single-anode soft x-ray source. In this case, titanium. The scan shows that the Ti L_α and L_η lines dominate over the continuum. When a line is selected, the monochromator is adjusted to operate at the line peak. The instrument is also equipped with a pair of filter wheels, each of which has enough holders to accomodate up to five witness samples. However, one holder of each wheel was intentionally left unoccupied so that x-ray spectra could be obtained without a filter in the x-ray detector beam path as part of the transmission measurement procedure. Spectra were acquired with a Manson model 851 gas-flow proportional counter equipped with a VYNS window, and which utilized either methane or P-10 as the fill gas.

4 Procedure

The procedure for making a transmission measurement involved obtaining a pair of filter-in/filter-out spectra, as well as a background spectrum. Once the background contribution was subtracted from both x-ray spectra, the value of the transmission simply involved dividing the number of remaining counts in the filter-in measurement by the number of remaining counts in the filter-out measurement. The measurement results are shown as the data points in figures 3 through 12.

5 Modelling the X-ray Transmission

A model of x-ray transmission for each witness sample was obtained by applying a nonlinear fitting routine (the Levenberg-Marquardt algorithm) to each data set. In fitting a model to the data, the mass areal densities of Al, C, N and O were adjusted in such a way as to minimize the reduced χ^2 value of the fit. The mass areal density of hydrogen was not incorporated into the analysis, as it makes a negligible contribution to the overall mass areal density of polyimide compared to the other elements. For the polypropylene window sample, only the mass areal density of carbon and the open area of the mesh supporting the window were adjusted. The calculations relied on the 1982 Henke values[4] as opposed to the 1993 values[5]. As discussed at the 1997 SPIE conference in San Diego[3], we believe that the 1993 Henke values for carbon and aluminum are suspect.

6 Results and Analysis

The mass areal densities of Al, C, N and O for each witness sample are listed in table 2. The reduced χ^2 values are included. The modelled transmission curve for each sample, along with the associated data set, is shown in figures 3 through 12. A plot of the relative residuals ($\frac{data-fit}{data}$) for one transmission curve is shown in figure 13.

In table 3, the derived aluminum thicknesses are compared to Luxel's quoted measurements. We assume that aluminum, when deposited in a thin layer, has a density of 2.50 g/cm^3.

By adding up the mass areal densities of C, N and O for any given witness sample, one obtains the mass areal density of polyimide. Dividing by the canonical density of polyimide, 1.40 g/cm^3, yields the thickness of the material. The mass areal density (and hence thickness) of polyimide is slightly underestimated, as the hydrogen mass areal density is not included in the thickness derivation. However, its contribution is negligible compared to the other three elements. The derived polyimide thickness of each sample is shown in table 4.

Based on the mass areal density of carbon for the proportional counter's polypropylene window sample (see table 1), the derived thickness is 1.13 ± 0.01 μm. The canonical density of polypropylene is 0.91 g/cm^3. The fit to the window's transmission measurements indicates that the mesh that gives the polypropylene its structural support has an open area of 0.838 ± 0.008.

7 Discussion

The derived aluminum thickness values for most of the witness samples agree with Luxel's measurements, within the limits of error. The derived aluminum thickness of witness samples TF101-1025, TF101-1044 and TF101-1154, however, do not compare as well with Luxel's values. The derived thickness values of these three shields, though, are within 2σ of Luxel's quoted values.

With respect to the polyimide results, the derived thickness values for all of the witness samples do agree well with Luxel's measurements, within the limits of error.

The thickness of the polypropylene used in our proportional counter windows is nominally given the value of 1.3 μm. The result of the analysis shows that the measured sample is 13% thinner than the nominal value.

8 Conclusion

We have carried out measurements on back-up, as well as flight, UV/ion shield witness samples using a monochromator equipped with an x-ray source. With a few exceptions, the derived thickness values of the samples are comparable to Luxel's reported measurements, within the limits of error.

The measured thickness of a sample of the polypropylene material used in our proportional counter windows is 13% thinner than the nominal 1.3 μm. Its mesh has an open area of 0.838 ± 0.008.

9 References

1. G.R. Meehan, A.T. Kenter, R.P. Kraft, S.S. Murray, M.V. Zombeck, K. Kobayashi, J.H. Chappell, M. Barbera, and A. Collura, "Measurement of the transmission of the UV/Ion Shields for the AXAF High Resolution Camera," Proc. SPIE, 2808, 1996.

2. Kraft, R. P., SAO Internal Memo, "Shadowgraph and transmission measurements of backup HRC-I UVIS", 1997 (hea-www.harvard.edu/HRC/calib/backup.html)

3. G.R. Meehan, S.S. Murray, M.V. Zombeck, R.P. Kraft, K. Kobayashi, J.H. Chappell, A.T. Kenter, M. Barbera, A. Collura, S. Serio, "Calibration of the UV/Ion Shields for the AXAF High Resolution Camera," Proc. SPIE, 3114, 1997 (http://hea-www.harvard.edu/HRC/calib/spie97.html)

4. B.L. Henke, *et al.*, *Atom. Data and Nucl. Data Tables*, 27, 1982.

5. B.L. Henke, E.M. Gullikson, and J.C. Davis, *Atom. Data and Nucl. Data Tables*, 54(2), 1993.

10 Tables and Figures

Witness Sample	Run Number	Material Composition	Shield Type and Flight Status
TF101-354	6569-8	Aluminum 305 ± 30Å Polyimide 1940 ± 100Å	UVIS-S Flight
TF101-891	6567-8	Aluminum 315 ± 30Å Polyimide 2040 ± 100Å Aluminum 1710 ± 50Å	UVIS-S Flight
TF101-1025	7018-8	Aluminum 300 ± 30Å Polyimide 2535 ± 100Å Aluminum 690 ± 50Å	UVIS-S (T) Flight Backup
TF101-1044	7018-8	Aluminum 300 ± 30Å Polyimide 2535 ± 100Å Aluminum 690 ± 50Å	UVIS-S (T) Flight Backup
TF101-1137	6982-8	Aluminum 755 ± 50Å Polyimide 5325 ± 100Å	UVIS-I Flight Backup
TF101-1154	6964-8	Aluminum 350 ± 35Å Polyimide 1980 ± 100Å Aluminum 1670 ± 50Å	UVIS-S (-1,+1) Flight Backup
TF101-1157	6964-8	Aluminum 350 ± 35Å Polyimide 1980 ± 100Å	UVIS-S (-1,+1) Flight Backup
TF101-1185	6982-8	Aluminum 755 ± 50Å Polyimide 5325 ± 100Å	UVIS-I Flight Backup
TF101-1220	7018-8	Aluminum 300 ± 30Å Polyimide 2535 ± 100Å	UVIS-S (T) Flight Backup
PC Window	N/A	1.3μm poly on 85% Mesh	N/A

Table 1. Description of the witness samples that were tested with the SAO x-ray monochromator. Witness samples TF101-354 and TF101-891 were also measured at the BESSY Synchrotron Light Source Facility. The nominal material composition and flight status of each filter is included. Included in this table is the material composition of the polypropylene used in the proportional counter (PC) window.

Witness Sample	Al (μg/cm^2)	C (μg/cm^2)	N (μg/cm^2)	O (μg/cm ^{2})	Reduced χ^2
TF101-354	6.73 ± 0.28	21.08 ± 0.74	1.73 ± 0.89	7.37 ± 0.67	2.455
TF101-891	49.55 ± 0.89	21.44 ± 1.05	2.06 ± 1.07	6.22 ± 1.24	2.989
TF101-1025	22.02 ± 0.42	25.52 ± 0.96	1.89 ± 1.27	9.86 ± 0.96	2.780
TF101-1044	21.88 ± 0.53	25.26 ± 0.87	1.98 ± 0.99	8.58 ± 1.18	3.516
TF101-1137	18.47 ± 0.55	54.06 ± 1.24	4.78 ± 1.28	13.75 ± 1.35	3.528
TF101-1154	45.27 ± 0.81	20.76 ± 1.01	1.70 ± 1.05	7.82 ± 1.24	1.838
TF101-1157	7.93 ± 0.42	20.98 ± 0.73	1.52 ± 0.89	5.91 ± 1.05	1.887
TF101-1185	18.51 ± 0.59	52.33 ± 1.49	5.58 ± 1.69	13.32 ± 1.76	5.531
TF101-1220	6.64 ± 0.27	26.14 ± 0.77	1.70 ± 0.92	8.13 ± 0.71	2.948
PC Window	N/A	103.0 ± 1.13	N/A	N/A	10.825

Table 2. The derived mass areal density of aluminum, and of the constituent elements of polyimide, for the UV/ion shield witness samples that were tested. The reduced χ^2 value for each fit is given, too. The polypropylene used in the proportional counter (PC) window is listed just with the mass areal density of carbon.

Witness Sample	Derived Aluminum Thickness Å	Luxel Measurement Å
TF101-354	269 ± 11	305 ± 30
TF101-891	1980 ± 35	2025 ± 58
TF101-1025	881 ± 16	990 ± 58
TF101-1044	875 ± 21	990 ± 58
TF101-1137	739 ± 22	755 ± 50
TF101-1154	1880 ± 32	2020 ± 61
TF101-1157	317 ± 16	350 ± 35
TF101-1185	740 ± 23	755 ± 50
TF101-1220	266 ± 10	300 ± 30

Table 3. The aluminum thickness value for each UV/ion shield witness sample as derived from the computed mass areal density of Al. Luxel's quoted values are included for comparison.

Witness Sample	Derived Polyimide Thickness $\AA$	Luxel Measurement $\AA$
TF101-354	2160 ± 164	1940 ± 100
TF101-891	2120 ± 240	2040 ± 100
TF101-1025	2660 ± 228	2535 ± 100
TF101-1044	2560 ± 217	2535 ± 100
TF101-1137	5180 ± 276	5325 ± 100
TF101-1154	2160 ± 236	1980 ± 100
TF101-1157	2030 ± 191	1980 ± 100
TF101-1185	5090 ± 353	5325 ± 100
TF101-1220	2570 ± 171	2535 ± 100

Table 4. The polyimide thickness value for each UV/ion shield witness sample as derived from the computed mass areal densities of C, N and O. Luxel's quoted values are included for comparison. Note that the derived polyimide thickness values are based on the best fit chemical composition and an assumed density of 1.40 g/cm^3.

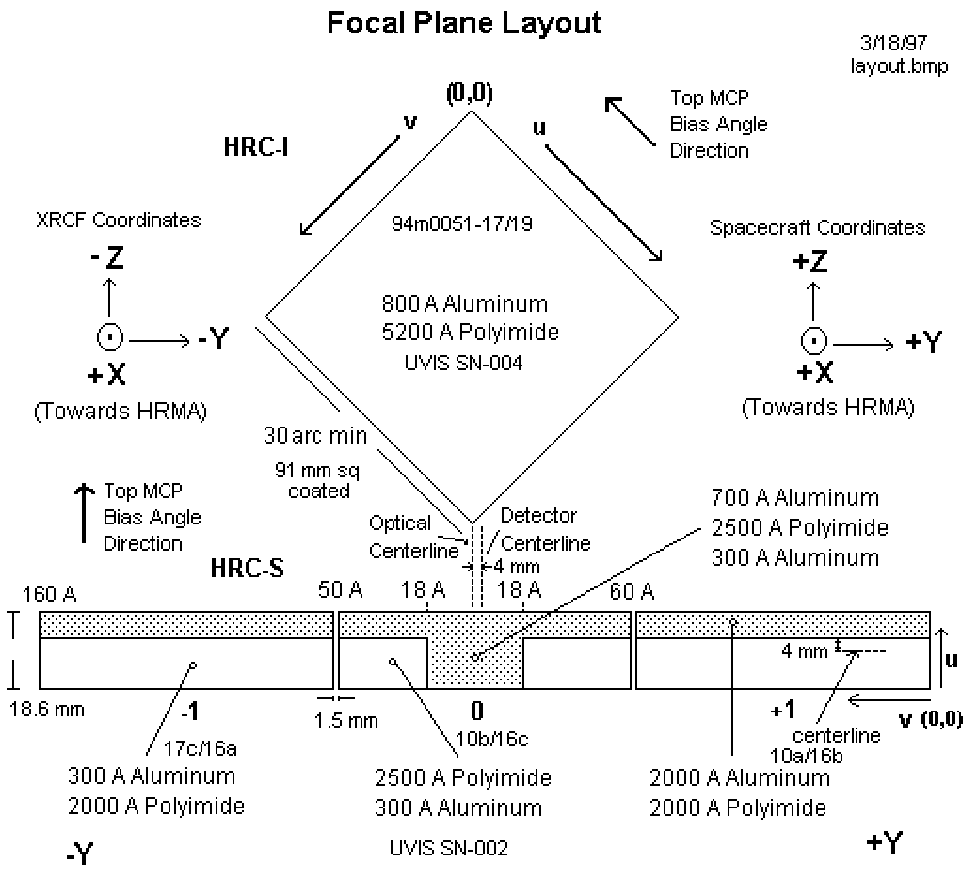

Figure 1: The material composition of the UVIS-I and UVIS-S are shown above. Where there is only a single side coated with aluminum, that side faces the High Resolution Mirror Assembly (HRMA) of AXAF. For the HRC-S Inner "T", it is the side with the 700Å coating that faces the HRMA. The figure also shows the relative orientation of the HRC-I and HRC-S in the instrument focal plane.

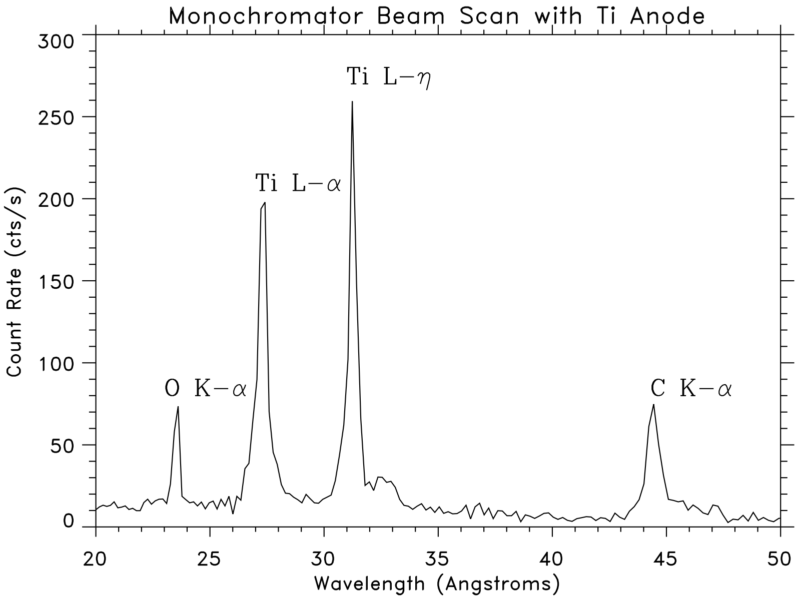

Figure 2: Example of a typical monochromator beam scan to identify the first order x-ray fluorescent lines associated with an anode. In this case, titanium. Note how the primary lines of interest, Ti L_α and L_η, dominate over the continuum.

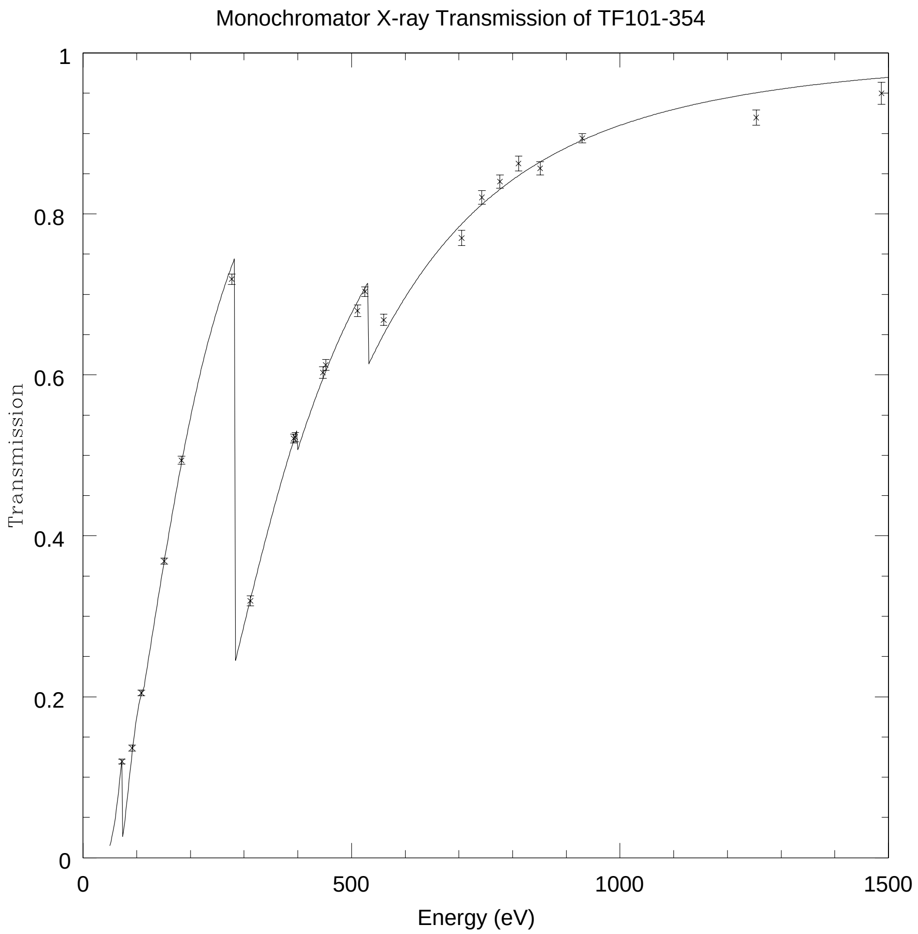

Figure 3: Modelled transmission curve for Luxel witness sample TF101-354 based on the monochromator data. The transmission measurements taken with the SAO x-ray monochromator are plotted, also.

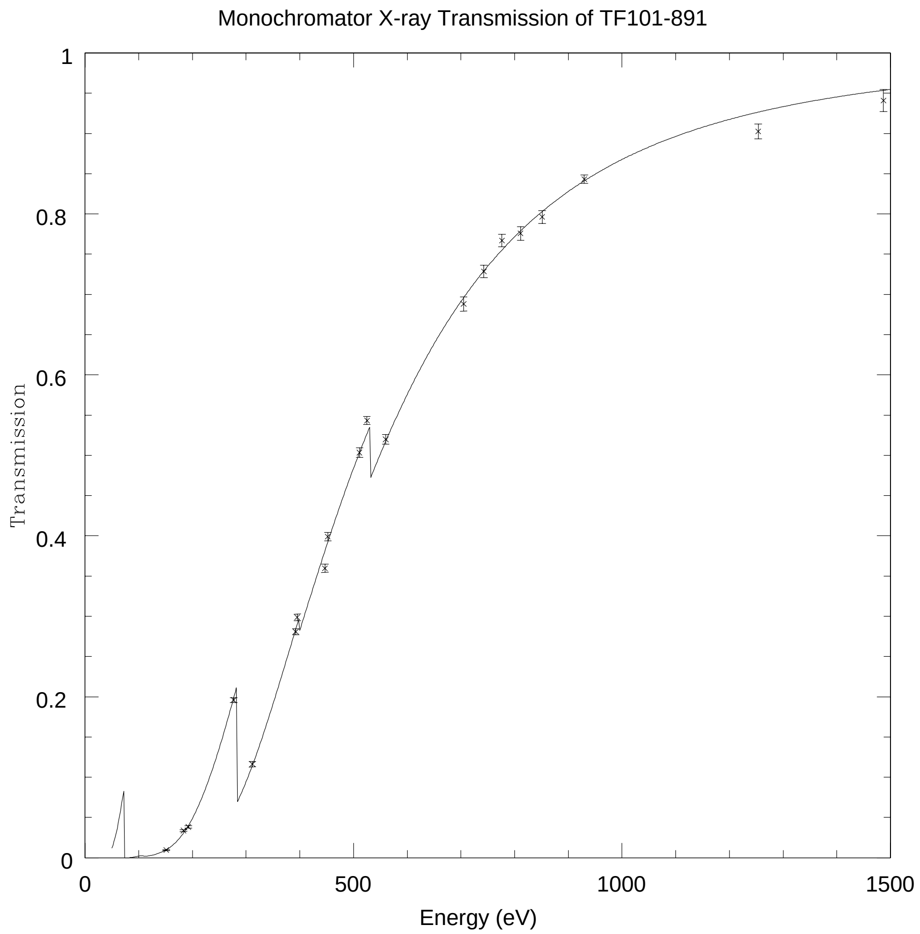

Figure 4: Modelled transmission curve for Luxel witness sample TF101-891 based on the monochromator data. The transmission measurements taken with the SAO x-ray monochromator are plotted, also.

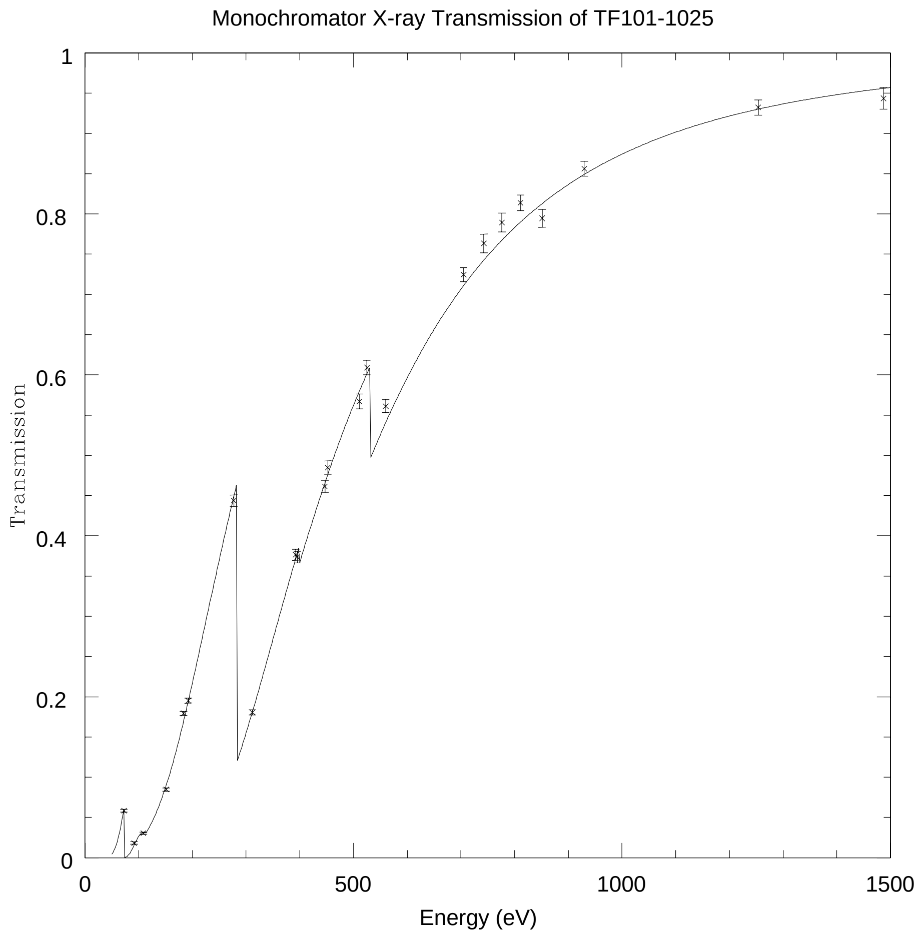

Figure 5: Modelled transmission curve for Luxel witness sample TF101-1025 based on the monochromator data. The transmission measurements taken with the SAO x-ray monochromator are plotted, also.

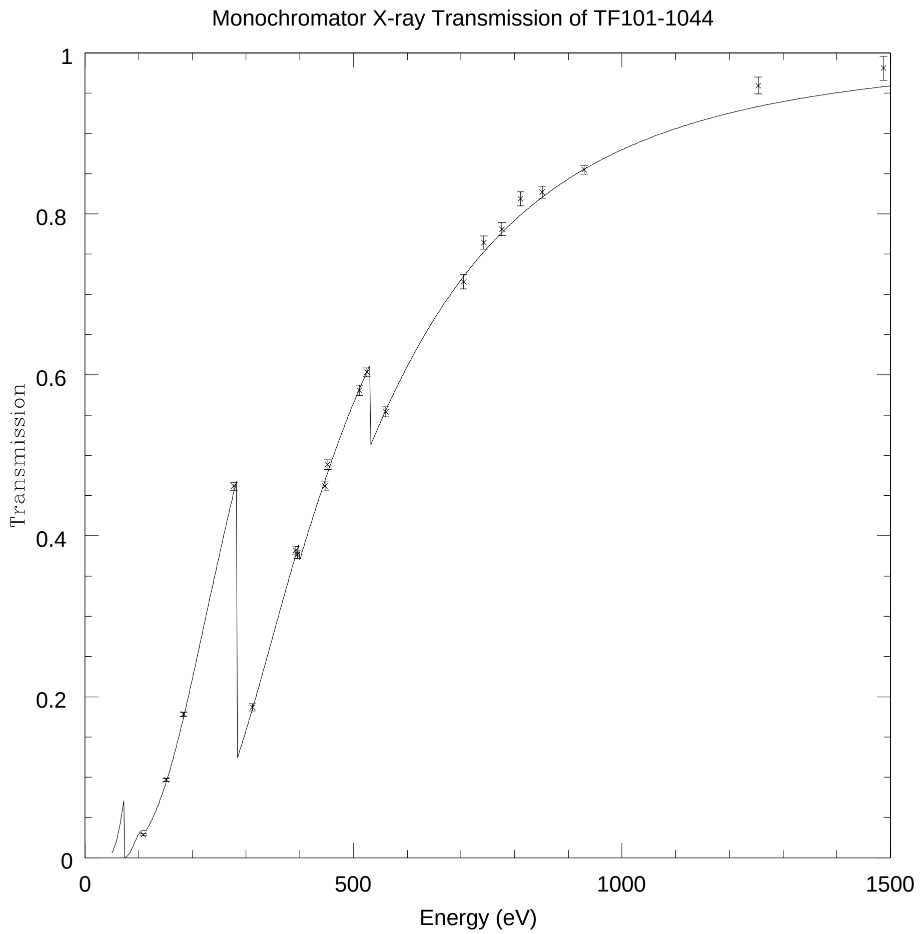

Figure 6: Modelled transmission curve for Luxel witness sample TF101-1044 based on the monochromator data. The transmission measurements taken with the SAO x-ray monochromator are plotted, also.

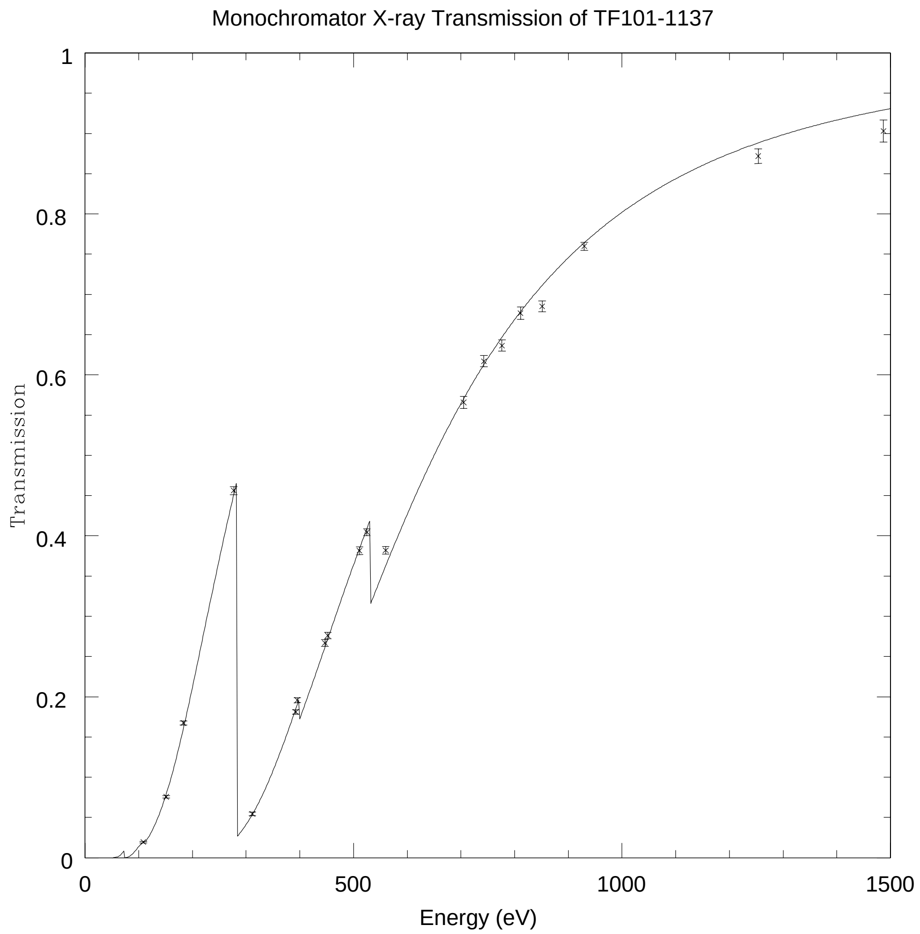

Figure 7: Modelled transmission curve for Luxel witness sample TF101-1137 based on the monochromator data. The transmission measurements taken with the SAO x-ray monochromator are plotted, also.

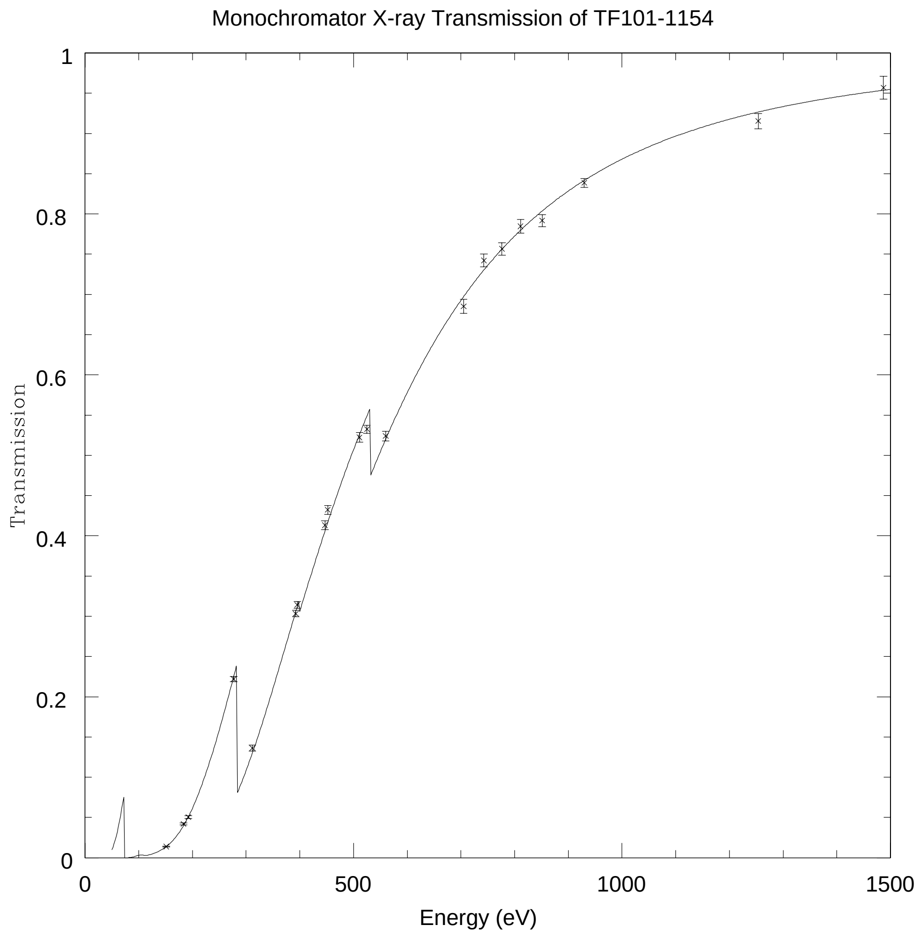

Figure 8: Modelled transmission curve for Luxel witness sample TF101-1154 based on the monochromator data. The transmission measurements taken with the SAO x-ray monochromator are plotted, also.

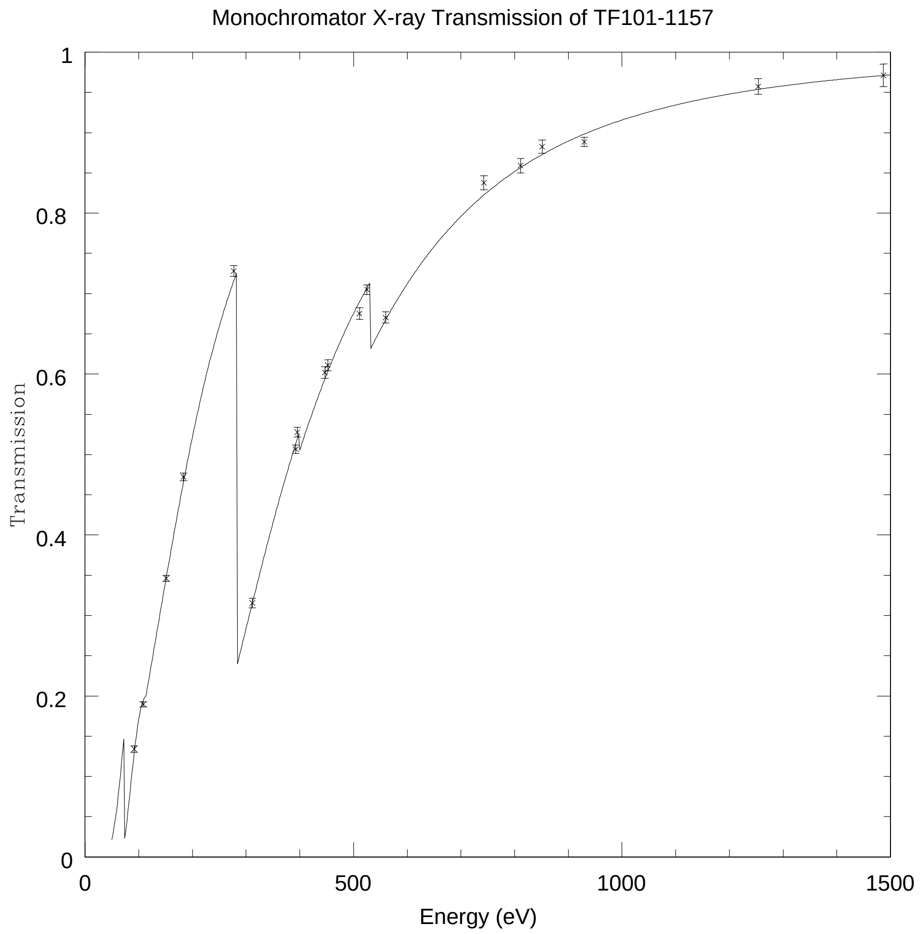

Figure 9: Modelled transmission curve for Luxel witness sample TF101-1157. The transmission measurements taken with the SAO x-ray monochromator are plotted, also.

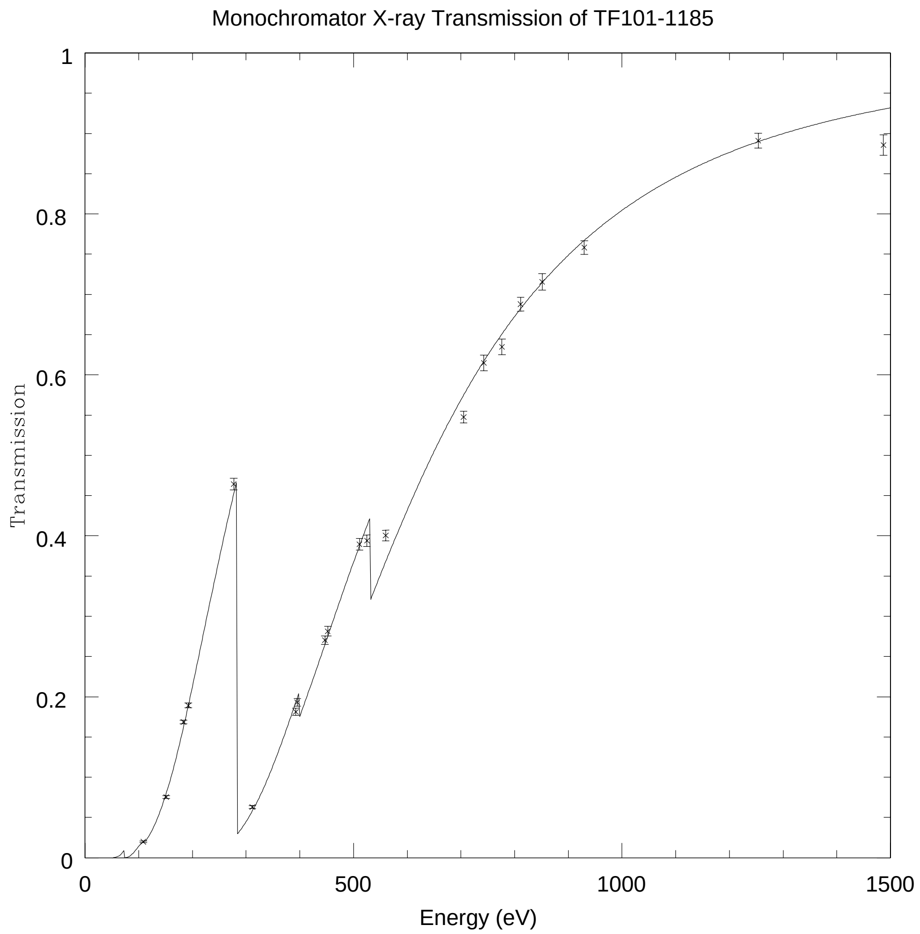

Figure 10: Modelled transmission curve for Luxel witness sample TF101-1185 based on the monochromator data. The transmission measurements taken with the SAO x-ray monochromator are plotted, also.

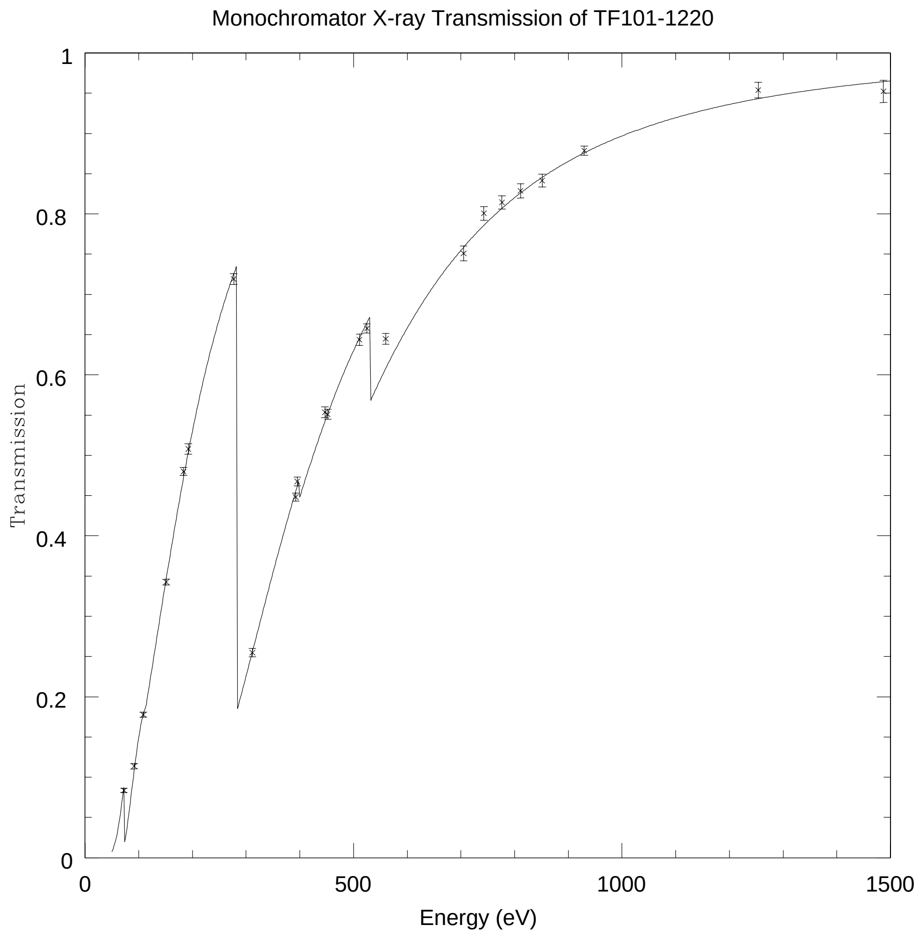

Figure 11: Modelled transmission curve for Luxel witness sample TF101-1220 based on the monochromator data. The transmission measurements taken with the SAO x-ray monochromator are plotted, also.

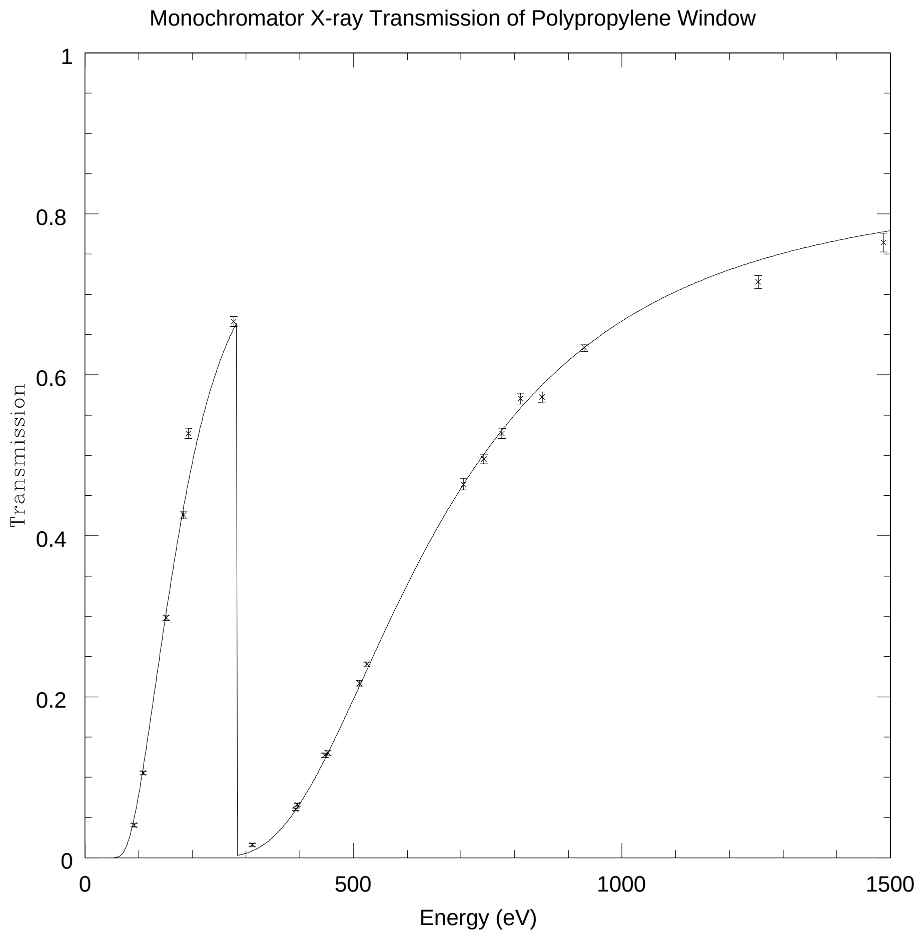

Figure 12: Modelled transmission curve for the polypropylene window sample used in the monitor detector based on the monochromator data. The transmission measurements taken with the SAO x-ray monochromator are plotted, also.

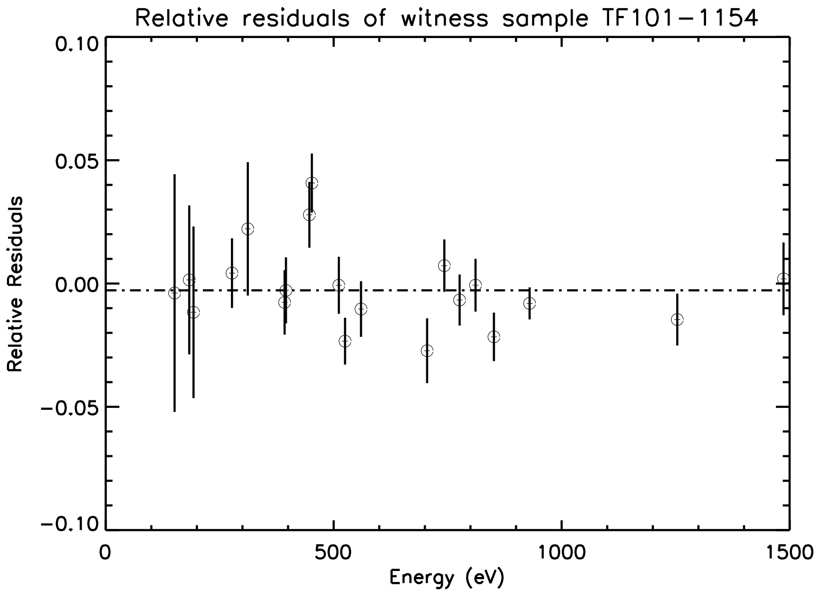

Figure 13: A plot of the relative residuals for witness sample TF101-1154, whose transmission was measured with the SAO x-ray monochromator. The fact that the median is close to zero indicates that there are no systematic errors.